

## Oxidation of Carbon Monoxide Cocatalyzed by Palladium(0) and the $H_5PV_2Mo_{10}O_{40}$ Polyoxometalate Probed by Electron Paramagnetic Resonance and Aerobic Catalysis

Hila Goldberg,<sup>†</sup> Ilia Kaminker,<sup>‡</sup> Daniella Goldfarb,<sup>‡</sup> and Ronny Neumann<sup>\*†</sup>

<sup>†</sup>Department of Organic Chemistry and <sup>‡</sup>Department of Chemical Physics and Weizmann Institute of Science, Rehovot, Israel 76100

Received May 5, 2009

The  $H_5PV_2Mo_{10}O_{40}$  polyoxometalate and  $Pd/Al_2O_3$  were used as co-catalysts under anaerobic conditions for the activation and oxidation of CO to  $CO_2$  by an electron transfer-oxygen transfer mechanism. Upon anaerobic reduction of  $H_5PV_2Mo_{10}O_{40}$  with CO in the presence of Pd(0) two paramagnetic species were observed and characterized by continuous wave electron paramagnetic resonance (CW-EPR) and hyperfine sublevel correlation (HYSCORE) spectroscopic measurements. Major species I (65–70%) is assigned to a species resembling a vanadyl cation that is supported on the polyoxometalate and showed a bonding interaction with  $^{13}CO$ . Minor species II (30–35%) is attributed to a reduced species where the vanadium(IV) atom is incorporated in the polyoxometalate framework but slightly distanced from the phosphate core. Under aerobic conditions,  $CO/O_2$ , a nucleophilic oxidant was formed as elucidated by oxidation of thianthrene oxide as a probe substrate. Oxidation reactions performed on terminal alkenes such as 1-octene yielded a complicated mixture of products that was, however, clearly a result of alkene epoxidation followed by subsequent reactions of the intermediate epoxide. The significant competing reaction was a hydro-carbonylation reaction that yielded a ~1:1 mixture of linear/branched carboxylic acids.

### Introduction

In the 1970–1980s, research demonstrated Pd(II) catalyzed oxidation reactions where phosphovanadomolybdates of the Keggin structure,  $[PV_xMo_{12-x}O_{40}]^{(3+x)-}$ , especially  $x = 2$ , were used as co-catalysts to reoxidize the primary palladium catalyst ultimately using molecular oxygen as terminal oxidant.<sup>1</sup> Over the years further reports of such aerobic catalytic oxidation reactions catalyzed by Pd/ $H_5PV_2Mo_{10}O_{40}$  have appeared,<sup>2</sup> together with many additional  $H_5PV_2Mo_{10}O_{40}$  catalyzed aerobic transformations and syntheses.<sup>3</sup> Recently,  $H_5PV_2Mo_{10}O_{40}$  has been used in metallorganic-polyoxometalate hybrid catalysts for aerobic oxidation of methane,<sup>4</sup> and formation of methyl ketones from alkenes with nitrous oxide.<sup>5</sup> On the mechanistic side some understanding has been developed suggesting that  $H_5PV_2Mo_{10}O_{40}$  catalyzed reactions

often proceed via electron transfer oxidation of the organic substrate,<sup>6</sup> which in some cases includes also oxygen transfer from the polyoxometalate to the organic substrate via an electron transfer-oxygen transfer.<sup>7</sup> In such reactions, there is first a electron transfer from the substrate to the  $H_5PV_2Mo_{10}O_{40}$  followed by oxygen transfer from the reduced polyoxometalate to the substrate, Scheme 1. For example, it has been shown in the case of anthracene oxidation that an outer sphere electron transfer (anthracene to polyoxometalate) leads to formation of an organic cation radical that should form cation radical-polyoxometalate ion pairs,<sup>8</sup> although such intermediate ion pairs have not been directly observed.

In parallel, there have been several recent reports wherein the combination of  $CO/O_2$  has been used in the presence of  $H_5PV_2Mo_{10}O_{40}$  and Pd to catalyze the hydroxylation or carboxylation of arenes to the corresponding phenols,<sup>9</sup> and the dicarboxylation of cyclic alkenes.<sup>10</sup> While Pd catalyzed

\*To whom correspondence should be addressed. E-mail: ronny.neumann@weizmann.ac.il.

(1) (a) Kozhevnikov, I. V.; Matveev, K. I. *Appl. Catal.* **1983**, *5*, 135–150. (b) Grate, J. H.; Hamm, D. R.; Mahajan, S. In *Catalysis of Organic Reactions*; Kosak, J. R., Johnson, T. A., Eds.; Marcel Dekker: New York, 1984; Chapter 16.

(2) Some key references: (a) Yokota, T.; Tani, M.; Sakaguchi, S.; Ishii, Y. *J. Am. Chem. Soc.* **2003**, *123*, 1476–1477. (b) Yokota, T.; Sakaguchi, S.; Ishii, Y. *Adv. Synth. Catal.* **2002**, *344*, 849–854. (c) Yamada, T.; Sakaguchi, S.; Ishii, Y. *J. Org. Chem.* **2005**, *70*, 5471–5474.

(3) (a) Hill, C. L.; Prosser-McCartha, C. M. *Coord. Chem. Rev.* **1995**, *143*, 407–455. (b) Kozhevnikov, I. V. *Chem. Rev.* **1998**, *98*, 171–198. (c) Neumann, R.; Khenkin, A. M. *Chem. Commun.* **2006**, 2529–2538.

(4) Bar-Nahum, I.; Khenkin, A. M.; Neumann, R. *J. Am. Chem. Soc.* **2004**, *126*, 10236–10237.

(5) Ettetdgui, J.; Neumann, R. *J. Am. Chem. Soc.* **2009**, *131*, 4–5.

(6) Neumann, R.; Levin, M. *J. Am. Chem. Soc.* **1992**, *114*, 7278–7286.

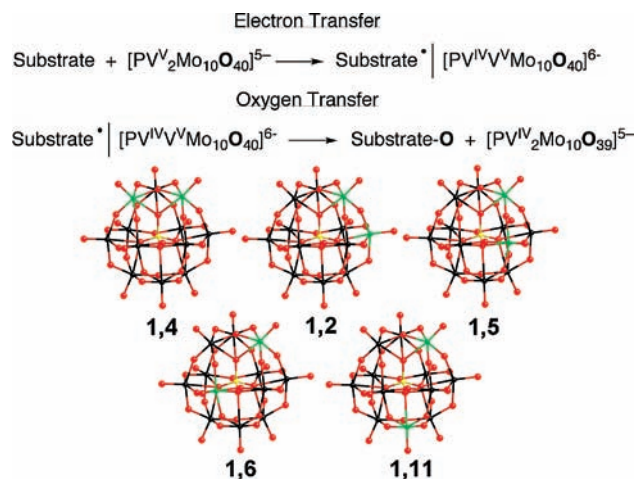
(7) (a) Khenkin, A. M.; Neumann, R. *Angew. Chem., Int. Ed.* **2000**, *39*, 4088–4090. (b) Khenkin, A. M.; Weiner, L.; Wang, Y.; Neumann, R. *J. Am. Chem. Soc.* **2001**, *123*, 8531–8542. (c) Khenkin, A. M.; Neumann, R. *J. Am. Chem. Soc.* **2008**, *130*, 14474–14476.

(8) Weinstock, I. A. *Chem. Rev.* **1998**, *98*, 113–170.

(9) (a) Tani, M.; Sakamoto, T.; Mita, S.; Sakaguchi, S.; Ishii, Y. *Angew. Chem., Int. Ed.* **2005**, *44*, 2586–2588. (b) Ohashi, S.; Sakaguchi, S.; Ishii, Y. *Chem. Commun.* **2005**, 486–487.

(10) Yokota, T.; Sakaguchi, S.; Ishii, Y. *J. Org. Chem.* **2002**, *67*, 5005–5008.

**Scheme 1.** General Pathway for an Electron Transfer–Oxygen Transfer Reaction and a Ball and Stick Representation of the Five Isomers of  $\text{H}_5\text{PV}_2\text{Mo}_{10}\text{O}_{40}$  (black, Mo; green, V; yellow, P; red, O)



oxidative carbonylation reactions have been often described in the literature,<sup>11</sup> such hydroxylation reactions are rare. Isotope labeling experiments ruled out the in situ formation of  $\text{H}_2\text{O}_2$  as oxidant by reduction of  $\text{O}_2$  by CO so that the nature and identity of the oxidizing species is still a question.<sup>9a</sup>

These intriguing recent CO/ $\text{O}_2$  hydroxylation reactions catalyzed by Pd(0)/ $\text{H}_5\text{PV}_2\text{Mo}_{10}\text{O}_{40}$  led us to study (a) the activation of CO in this catalytic system and (b) the reaction of activated CO with  $\text{O}_2$  emphasizing the reactivity of the oxidizing species obtained. We found by X-band HYSCORE (hyperfine sublevel correlation) measurements, under anaerobic conditions, that CO reacted with  $\text{H}_5\text{PV}_2\text{Mo}_{10}\text{O}_{40}$  in the presence of Pd(0) and formed  $\text{V}^{\text{IV}}\text{-CO}$  complexes by electron transfer. Furthermore, these  $\text{V}^{\text{IV}}\text{-CO}$  complexes react via oxygen transfer from the polyoxometalate to yield  $\text{CO}_2$ . Under aerobic conditions, these  $\text{V}^{\text{IV}}\text{-CO}$  complexes appear to yield a nucleophilic oxygen donating intermediate that can also epoxidize terminal alkenes.

## Results and Discussion

**Anaerobic Oxidation of CO.** Dissolution of 5  $\mu\text{mol}$   $\text{H}_5\text{PV}_2\text{Mo}_{10}\text{O}_{40}$  (orange color, oxidized form) in 1 mL 9:1 AcOH/ $\text{H}_2\text{O}$  as solvent followed by addition of 2 bar CO in a 25 mL glass pressure tube at 90 °C for 5 h showed no evidence of oxidation of CO to  $\text{CO}_2$  as analyzed by gas chromatography (GC) or formation of reduced  $\text{H}_5\text{PV}_2\text{Mo}_{10}\text{O}_{40}$  via appearance of the signature heteropoly blue. Addition of 5% Pd/ $\text{Al}_2\text{O}_3$  (1  $\mu\text{mol}$  Pd) to such a reaction mixture did lead to the formation of a stoichiometric amount of  $\text{CO}_2$  and formation of reduced, blue  $\text{H}_5\text{PV}_2\text{Mo}_{10}\text{O}_{40}$ . This anaerobic oxidation of CO to  $\text{CO}_2$  over a period of 5 h in the presence of both  $\text{H}_5\text{PV}_2\text{Mo}_{10}\text{O}_{40}$  and 5% Pd/ $\text{Al}_2\text{O}_3$  was verified in two ways. First, by carrying out the CO oxidation with  $\sim 50\%$   $^{18}\text{O}$  labeled  $\text{H}_5\text{PV}_2\text{Mo}_{10}\text{O}_{40}$  to yield  $\text{C}^{16}\text{O}^{18}\text{O}$  as measured by GC-MS and second by using  $^{13}\text{C}$  and observing the formation of  $^{13}\text{CO}_2$  by  $^{13}\text{C}$  NMR at 125 ppm. Importantly also there was

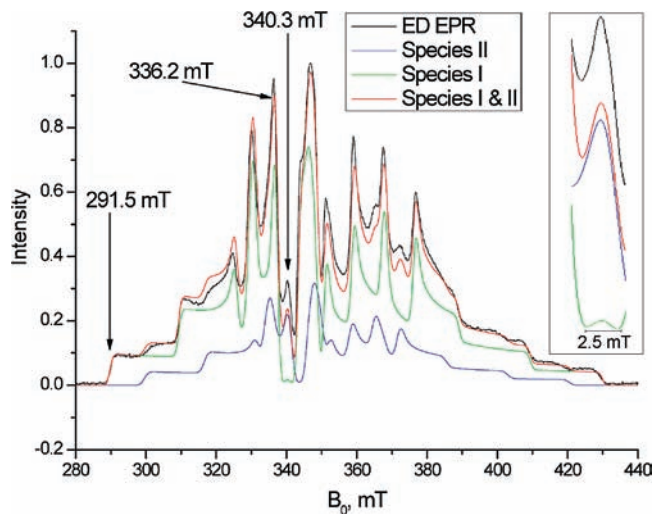


**Figure 1.** ED EPR spectrum (black) of  $\text{H}_5\text{PV}_2\text{Mo}_{10}\text{O}_{40}$  reacted with CO in the presence of Pd/ $\text{Al}_2\text{O}_3$  and simulations obtained with the parameters listed in Table 1. The individual traces of the two species (I-green, II-blue) and their sum (red) are presented. Inset: expanded spectra at 340.3 mT.

no evidence of a redox reaction between  $\text{H}_5\text{PV}_2\text{Mo}_{10}\text{O}_{40}$  and Pd/ $\text{Al}_2\text{O}_3$  in a reaction carried out in the absence of CO. These results allow a conclusion consistent with previous mechanistic studies on the oxidation of anthracene and primary alcohols<sup>7</sup> that CO activated by Pd(0) leads to an electron transfer-oxygen transfer reaction wherein the polyoxometalate is reduced and CO is oxidized to  $\text{CO}_2$  via oxygen transfer from  $\text{H}_5\text{PV}_2\text{Mo}_{10}\text{O}_{40}$  to CO. It should be noted that Pd/C showed similar reactivity to Pd/ $\text{Al}_2\text{O}_3$ ; Pt/ $\text{Al}_2\text{O}_3$ , Ru/ $\text{Al}_2\text{O}_3$  and Rh/ $\text{Al}_2\text{O}_3$  were all inactive.

**EPR Measurements.** The anaerobic reaction of  $^{13}\text{C}$  CO activated by Pd(0) with  $\text{H}_5\text{PV}_2\text{Mo}_{10}\text{O}_{40}$  was further probed by X-band echo detected (ED) EPR. A solution of 5 mM  $\text{H}_5\text{PV}_2\text{Mo}_{10}\text{O}_{40}$  and 5% Pd/ $\text{Al}_2\text{O}_3$  (1 mg) in 8:1:1 AcOH/ $\text{H}_2\text{O}$ /glycerol was gently heated ( $\sim 35$  °C, 10 min) under  $\sim 1$  bar  $^{13}\text{C}$  CO to form the reduced polyoxometalate; the mild conditions used prevented formation of  $\text{CO}_2$ . The ED-EPR spectrum of Pd activated  $^{13}\text{C}$  CO with  $\text{H}_5\text{PV}_2\text{Mo}_{10}\text{O}_{40}$ , shown in Figure 1 clearly shows the formation of two reduced polyoxometalate species. The EPR parameters and the relative amounts of the two species were determined from simulations, also shown in Figure 1; the simulation parameters are given in Table 1. The EPR parameters of species I are similar to those of a vanadyl cation,  $\text{VO}^{2+}$  from  $\text{VO}(\text{acac})_2$ , in aqueous solution and are listed in Table 1 as well.

HYSCORE measurements at different observer magnetic fields along the EPR powder pattern were carried out to obtain details on the near environment of the reduced  $\text{V}^{\text{IV}}$  atom in the two species and more specifically to observe interaction of  $^{13}\text{C}$  CO with the polyoxometalate. Figure 2a shows the spectrum recorded at 291.5 mT. At this field only species I contributes to the EPR signal, and the spectrum is “single crystal-like” (Figure 1). The spectrum shows a ridge with a width of 1.4 MHz centered at the  $^{13}\text{C}$  Larmor frequency,  $\nu_L(^{13}\text{C}) = 3.12$  MHz. In addition, intense  $^1\text{H}$  ridges from the solvent and  $\text{H}_5\text{PV}_2\text{Mo}_{10}\text{O}_{40}$  are observed. The extent of the  $^1\text{H}$  ridges (8.4 MHz) indicates a large dipolar interaction characteristic

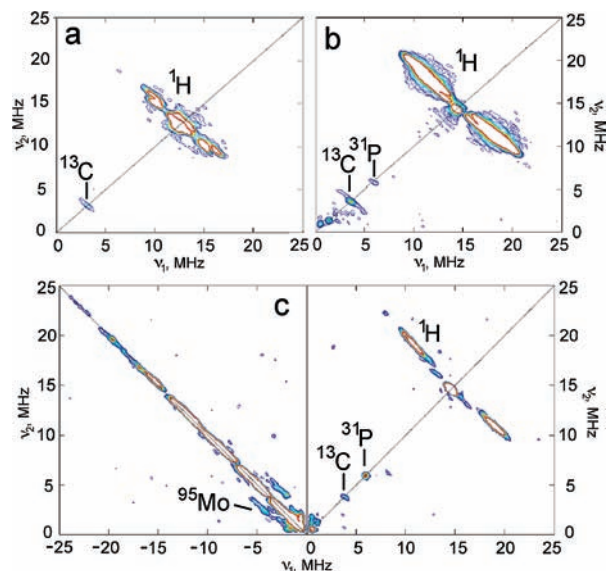
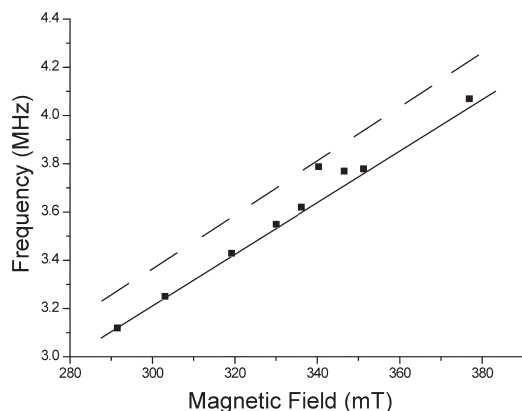
(11) (a) Tsuji, J. *Palladium Reagents, Innovations in Organic Synthesis*; Wiley: Chichester, 1995. (b) Herrmann, W. A. In *Applied Homogeneous Catalysis with Organometallic Complexes*; Cornils, B., Herrmann, W. A., Eds.; VCH: Weinheim, 1996; Volume II, pp 712–732.

**Table 1.** EPR Parameters for  $\text{H}_5\text{PV}_2\text{Mo}_{10}\text{O}_{40}$  Reacted with  $^{13}\text{C}$  in the Presence of  $\text{Pd}/\text{Al}_2\text{O}_3$ 

|                      | species I | species II | VO(acac) <sub>2</sub> |
|----------------------|-----------|------------|-----------------------|
| % abundance          | 65–70     | 30–35      |                       |
| $A_{\parallel}$ , mT | 19.5      | 16.8       | 18.9                  |
| $A_{\perp}$ , mT     | 7.1       | 5.7        | 7.1                   |
| $g_{\parallel}$      | 1.944     | 1.943      | 1.938                 |
| $g_{\perp}$          | 1.989     | 1.986      | 1.978                 |

of equatorial water ligands.<sup>12–14</sup> Interestingly, no signals of  $^{31}\text{P}$  were observed indicating a long P–V distance. The HYSCORE spectrum taken at 336.2 mT, Figure 2b, has contributions from both species, but species I dominates. Here we observe a clear ridge of a width of 2.8 MHz that crosses the diagonal at  $\nu_{\text{I}}(^{13}\text{C}) = 3.25$  MHz. At this field position the orientation selection is negligible, and the width of the ridge can be considered as the largest  $^{13}\text{C}$  hyperfine interaction,  $A_{\parallel}$ . Neglecting any isotropic hyperfine interaction,  $a_{\text{iso}}$ , and using the point dipole approximation a minimum C–V distance of 2.42 Å is estimated indicating a direct coordination of  $^{13}\text{C}$  to  $\text{V}^{\text{IV}}$ . The presence of a significant  $a_{\text{iso}}$  value will of course change the estimated distance on the one hand, but still provide additional experimental evidence for direct coordination. The spectrum also shows a peak on the diagonal at 5.85 MHz, which corresponds to the  $^{31}\text{P}$  Larmor frequency,  $\nu_{\text{I}}(^{31}\text{P})$ . It has a width of 0.6 MHz, from which a minimum distance P–V of 4.75 Å is estimated. Because of the absence of a  $^{31}\text{P}$  signal at 291.5 mT, where only species I contributes to the echo, we assign the observed  $^{31}\text{P}$  signal at this field to species II. The extent of the  $^1\text{H}$  ridges (12.3 MHz) indicates a large dipolar interaction, typical of equatorial water ligands.<sup>12–14</sup>

At 340.3 mT, Figure 2c, where the contribution of species II dominates (see Figure 1, inset) signals of  $^{31}\text{P}$  and  $^1\text{H}$  are detected in the (+, +) quadrant. A close look at the (–, +) quadrant reveals two ridges parallel to the diagonal with a width of 2.74 MHz and a frequency spacing of 1.9 MHz, corresponding to the twice the Larmor frequency of  $^{95}\text{Mo}$ ,  $\nu_{\text{I}}(^{95}\text{Mo})$ , ( $I = 5/2$ , natural abundance 15.9%). The assignment was made to the  $^{95}\text{Mo}$  isotope because although the  $^{97}\text{Mo}$  isotope has a similar Larmor frequency, it has a lower natural abundance and a significantly larger quadrupole moment that should lead to extensive broadening. From the length of the ridges and assuming an axial hyperfine interaction,  $A_{\perp} \sim 4.5$  MHz and  $A_{\parallel} \sim 9$  MHz can be estimated. In addition a signal on the diagonal appears at 3.79 MHz, which is close to  $\nu_{\text{I}}(^{13}\text{C})$  at this field, but shifted upfield by about 0.1 MHz, suggesting that it could arise from  $^{51}\text{V}$  and not  $^{13}\text{C}$ . To substantiate this assignment we plotted the position of this peak as a function of magnetic field for all recorded HYSCORE spectra, and the result is shown in Figure 3, along with the expected  $\nu_{\text{I}}(^{13}\text{C})$  and  $^{51}\text{V}$  Larmor,  $\nu_{\text{I}}(^{51}\text{V})$ , frequencies. At all fields where species I dominates, the frequency of this peak falls on the  $\nu_{\text{I}}(^{13}\text{C})$  line; however, around 340 mT where species II dominates, it deviated from this line, and at 340.3 mT it falls on the  $\nu_{\text{I}}(^{51}\text{V})$  line.

**Figure 2.** HYSCORE spectra recorded at (a) 291.5, (b) 336.2, and (c) 340.3 mT. The peaks on the diagonal of the (–, +) quadrant are noise due to incomplete removal of unwanted echoes by the phase cycle.**Figure 3.** Plots of the frequency of the HYSCORE diagonal peak in the (+, +) quadrant in the region of 3.5 MHz as a function of the observer magnetic field. The solid and dashed lines correspond to  $\nu_{\text{I}}(^{13}\text{C})$  and  $\nu_{\text{I}}(^{51}\text{V})$ , respectively.

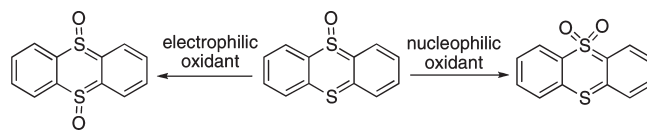
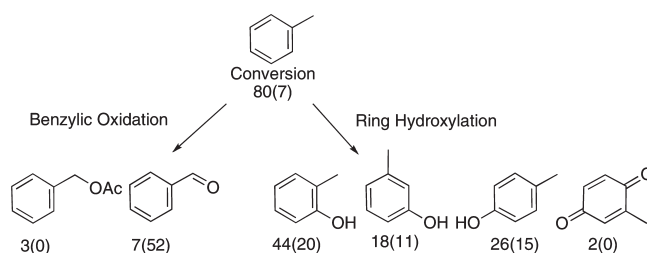
From the HYSCORE results we conclude that species I has a vanadium(IV) site that is similar to a vanadyl cation and has a  $^{13}\text{C}$  atom in its close vicinity ( $\sim 2.4$  Å). The proximity of the  $^{13}\text{C}$  atom to the  $\text{V}^{\text{IV}}$  site is the first strong spectral evidence for a previously hypothesized bonding interaction of a substrate, in this case  $^{13}\text{C}$  after activation with Pd, with  $\text{H}_5\text{PV}_2\text{Mo}_{10}\text{O}_{40}$ , Scheme 1. This bonding interaction follows electron transfer from the  $^{13}\text{C}$  to  $\text{H}_5\text{PV}_2\text{Mo}_{10}\text{O}_{40}$  to yield  $\text{H}_5\text{PV}^{\text{IV}}\text{V}^{\text{V}}\text{Mo}_{10}\text{O}_{40}\cdot\text{CO}$ . The vanadium(IV) is rather remote from the  $\text{PO}_4^{3-}$  core and the molybdenum atoms (no  $^{31}\text{P}$  and  $^{95}\text{Mo}$  signals) of the polyoxometalate and can be considered to be supported on the polyoxometalate. Furthermore, the observation of the  $^{13}\text{C}$  extended ridges at the  $g_{\perp}$  region and a small coupling along  $g_{\parallel}$  suggests that the  $^{13}\text{C}$  atom is in the equatorial plane. In contrast, in species II the vanadium(IV) atom has  $^{31}\text{P}$ ,  $^{95}\text{Mo}$ , and  $^{51}\text{V}$  atoms in its close vicinity, but not a  $^{13}\text{C}$  atom. Hence, species II is assigned as one where the vanadium(IV) is incorporated in the polyoxometalate. This assignment is also consistent with

(12) van Willigen, H. *J. Magn. Reson.* **1980**, *39*, 37–46.(13) Atherton, N. M.; Shackleton, J. F. *Mol. Phys.* **1980**, *39*, 1471–1485.(14) Dikanov, S. A.; Liboiron, B. D.; Orvig, C. *J. Am. Chem. Soc.* **2002**, *124*, 2969–2978.

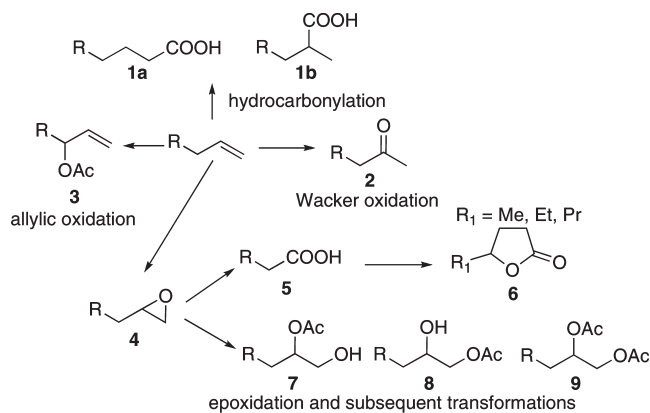
the smaller  $A_{||}$  of species II compared to species I. The contribution of each of the equatorial ligands to the value of  $A_{||}$  for  $^{51}\text{V}$  correlates approximately inversely with the electron donor capacity of the ligand, with the most donating ligands contributing the least to the hyperfine coupling.<sup>15</sup> In  $\text{H}_5\text{PV}^{IV}\text{V}^{IV}\text{Mo}_{10}\text{O}_{40}$  the equatorial ligands, that is, the bridging oxo groups of the polyoxometalate, are high in charge and electron donating.<sup>16</sup> The equatorial ligands to vanadium(IV) incorporated in the polyoxometalate also should exhibit some deviation from planarity, but it has been shown that the effect of such a distortion on the  $A_{||}$  is rather small.<sup>17</sup> One should, however, note that from crystal structures of the oxidized species the V–P distance is  $\sim 3.5$  Å whereas the experimentally estimated distance for the reduced species II is longer (4.75 Å). It is likely that the strong tendency of vanadium(IV) to adapt a square pyramidal rather than octahedral coordination leads to its tendency to be removed from the polyoxometalate framework, yet the large  $^{95}\text{Mo}$  hyperfine couplings confirms its equatorial position relative to vanadium(IV), and the weak  $^{31}\text{P}$  coupling to vanadium(IV) confirms its axial location,<sup>14</sup> as expected from the Keggin structure. Moreover, the weak  $^{51}\text{V}$  hyperfine coupling indicates that species II corresponds to the 1,6 and 1,11 isomers of  $\text{H}_5\text{PV}_2\text{Mo}_{10}\text{O}_{40}$  where the two vanadium atoms are not nearest neighbors, Scheme 1. Otherwise a hyperfine interaction comparable to that observed for  $^{95}\text{Mo}$  would have been expected. Also notable in the context of formation of two species in a *wet solution* in this study is a previous study on the vanadium coordination environment in hydrated and dehydrated *solid*  $\text{H}_4\text{PVMo}_{11}\text{O}_{40}$  where water of hydration removed the vanadium(IV) atom from the polyoxometalate to an interstitial position.<sup>18</sup> There ENDOR of the dehydrated gave a P–V distance of 4.2 Å and the species was assigned to  $\text{VO}^{2+}$  directly attached or coordinated to the surface oxygen atoms of the Keggin species. Apparently, the solution and solid phase structures of reduced vanadium(IV) containing polyoxomolybdates are different.

**Aerobic Oxidations.** As stated above, the identity and mode of action of the active oxidant formed from a mixture of  $\text{CO}/\text{O}_2$  in the presence of Pd and  $\text{H}_5\text{PV}_2\text{Mo}_{10}\text{O}_{40}$  remains a question. First, to study whether a nucleophilic or electrophilic oxidant is formed we used thianthrene oxide as a probe substrate, Scheme 2.<sup>19</sup> Thus, a reaction of 270  $\mu\text{mol}$  thianthrene oxide with 7 bar CO and 3 bar  $\text{O}_2$  catalyzed by 10  $\mu\text{mol}$   $\text{H}_5\text{PV}_2\text{Mo}_{10}\text{O}_{40}$  and 1  $\mu\text{mol}$  Pd (5% Pd/ $\text{Al}_2\text{O}_3$ ) in 1.5 mL 9:1 AcOH/ $\text{H}_2\text{O}$  with 0.1 mmol AcONa at 90 °C for 15 h yielded only 95  $\mu\text{mol}$  sulfone indicating a reactive nucleophilic oxidant is operative.

Furthermore, using 1 mmol toluene as substrate under otherwise identical reactions conditions as above yielded 90% arene ring hydroxylation products at 80% conversion with strong suppression of autoxidation at the

**Scheme 2.** Oxidation of Thianthrene Oxide**Scheme 3.** Benzylic versus Aromatic Oxidation of Toluene with  $\text{CO}/\text{O}_2$  Catalyzed by Pd/ $\text{Al}_2\text{O}_3$  and  $\text{H}_5\text{PV}_2\text{Mo}_{10}\text{O}_{40}$ <sup>a</sup>

<sup>a</sup> Values in parentheses are for the reaction without Pd/ $\text{Al}_2\text{O}_3$ .

**Chart 1.** Reaction Pathways for the Reaction of 1-octene ( $\text{R} = n$ -pentyl) with  $\text{CO}/\text{O}_2$  Catalyzed by Pd/ $\text{Al}_2\text{O}_3$  and  $\text{H}_5\text{PV}_2\text{Mo}_{10}\text{O}_{40}$ 

| Conversion - 97% | Compound       | 1a/1b | 2   | 3 | 4 | 5   | 6  | 7 | 8  | 9 |    |
|------------------|----------------|-------|-----|---|---|-----|----|---|----|---|----|
|                  | Selectivity, % | 40    | 1:1 | 1 | 2 | --- | 10 | 5 | 16 | 9 | 15 |

<sup>a</sup> Reaction conditions - 1 mmol 1-octene, 7 bar CO, 3 bar  $\text{O}_2$ , 10  $\mu\text{mol}$   $\text{H}_5\text{PV}_2\text{Mo}_{10}\text{O}_{40}$ , 1  $\mu\text{mol}$  Pd (5% Pd/ $\text{Al}_2\text{O}_3$ ) in 1.5 mL 9:1 AcOH/ $\text{H}_2\text{O}$ , 0.1 mmol AcONa at 90 °C for 15 h. Products were identified using reference samples and GC-MS and quantified using GC. About 30% of the CO is oxidized to  $\text{CO}_2$ . Reactions with different palladium sources and alternative solvent compositions, and various terminal alkenes are presented in Supporting Information, Tables S1–S3.

benzylic position, Scheme 3. The importance of Pd in the activation of CO and also the direction of reaction toward ring hydroxylation versus benzylic autoxidation is prominent. Finally, the reactivity of terminal alkenes such as 1-octene with this catalytic system was most informative despite the rather complicated mixture of products obtained, Chart 1.

The results show importantly that the Wacker reaction previously reported to be catalyzed by Pd(II)/  $\text{H}_5\text{PV}_2\text{Mo}_{10}\text{O}_{40}$  in the presence of chloride was suppressed,<sup>2</sup> as was the autoxidative allylic oxidation. Two major pathways for the transformation of 1-octene were observed. The first, about 40% of the products, yielded a  $\sim 1:1$  ratio of nonanoic, **1a**, and 2-methyloctanoic, **1b**, acids. The formation of the saturated carboxylic acids rather than unsaturated acids or dicarboxylic acids indicates that a

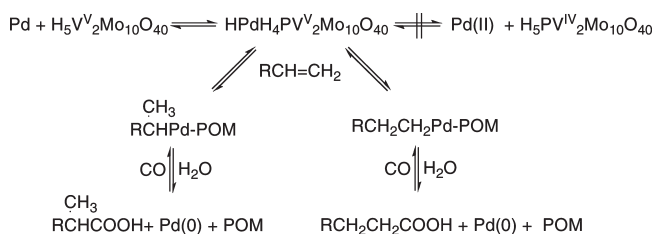
(15) Smith, T. S.; LoBrutto, R.; Pecoraro, V. L. *Coord. Chem. Rev.* **2002**, *228*, 1–18.

(16) Hirao, H.; Kumar, D.; Chen, H.; Neumann, R.; Shaik, S. *J. Phys. Chem. C* **2007**, *111*, 7711–7719.

(17) Cornman, C. R.; Geiser, K. M.; Rowley, S. P.; Boyle, P. D. *Inorg. Chem.* **1997**, *36*, 6401–6408.

(18) Pöpl, A.; Manikandan, P.; Köhler, K.; Maas, P.; Strauch, P.; Bötcher, R.; Goldfarb, D. *J. Am. Chem. Soc.* **2001**, *123*, 4577–4584.

(19) (a) Adam, W.; Haas, W.; Lohray, B. B. *J. Am. Chem. Soc.* **1991**, *113*, 6202–6208. (b) Adam, W.; Golsch, D. *Chem. Ber.* **1994**, *127*, 1111–1113.

**Scheme 4.** Formation of Carboxylic Acids by Hydrocarbonylation

Pd(0) catalyzed hydrocarbonylation reaction rather than a Pd(II) oxidative carbonylation reaction is operative,<sup>20</sup> Scheme 4. Oxidative addition of the acidic  $\text{H}_5\text{PV}_2\text{Mo}_{10}\text{O}_{40}$  and insertion of the alkene and CO in the presence of  $\text{H}_2\text{O}$  yielded the carboxylic acids. The second reaction pathway, about 55% of products, was the result of epoxidation and subsequent transformations, Chart 1. Thus, although the original epoxidation product, 1-octene oxide, **4**, was not directly observed because of its apparent short lifetime under reaction conditions, its use as a substrate under the same reaction conditions gave *exactly* the same product ratios for **5–9** as observed in the reaction of 1-octene. The known transformations of **4** (ring-opening and esterification, and C–C bond cleavage) are primarily due to the acidic conditions dictated by the polyoxometalate.<sup>21</sup>

The formation of furanones deserved specific verification and comment. Therefore, the reaction of heptanoic acid as substrate (1 mmol heptanoic acid, 7 bar CO, 3 bar  $\text{O}_2$ , 10  $\mu\text{mol}$   $\text{H}_5\text{PV}_2\text{Mo}_{10}\text{O}_{40}$ , 1  $\mu\text{mol}$  Pd (5% Pd/ $\text{Al}_2\text{O}_3$ ) in 1.5 mL 9:1 AcOH/ $\text{H}_2\text{O}$ , 0.1 mmol AcONa, 90 °C, 15 h) showed a 11% conversion with formation of 2-methyl-, 2-ethyl-, and 2-propylfuranone in an approximately ~3:1:1 ratio. Such activation of remote C–H bonds in aliphatic carboxylic acids has been reported in the past to be catalyzed by Pt(II) using Pt(IV) as oxidant.<sup>22</sup> Assumably,  $\text{H}_5\text{PV}_2\text{Mo}_{10}\text{O}_{40}$  serves here as oxidant in this reaction catalyzed by Pd(II).<sup>4,5</sup>

**Mechanistic Discussion.** From the combined EPR spectroscopy and catalysis studies several hypotheses may be suggested concerning (i) the reduced  $\text{H}_5\text{PV}_2\text{Mo}_{10}\text{O}_{40}$  species, (ii) the reaction of  $\text{H}_5\text{PV}_2\text{Mo}_{10}\text{O}_{40}$  with CO activated by Pd(0), and (iii) the reactivity of  $\text{H}_5\text{PV}_2\text{Mo}_{10}\text{O}_{40}$ /Pd(0) activated CO under anaerobic and aerobic conditions. The EPR measurements show that two different types of species were formed upon reduction of  $\text{H}_5\text{PV}_2\text{Mo}_{10}\text{O}_{40}$  with CO. Major species I showed CO bonded to a vanadium(IV) atom that is remote or supported on the polyoxometalate cluster as indicated by the absence of coupling to phosphorus and molybdenum atoms. Minor species II does not appear to bind CO, and the vanadium(IV) atom appears to be incorporated within the polyoxometalate cluster as indicated by the presence of an axial phosphorus atom and equatorial molybdenum atoms but slightly distanced from the  $\text{PO}_4^{3-}$  core. Species II can be associated with  $\text{H}_5\text{PV}_2\text{Mo}_{10}\text{O}_{40}$  isomers with distal vanadium sites in the oxidized state. The fact that CO was observed at low

temperature to be bonded only to the vanadium(IV) atom supported on the polyoxometalate leads to the possibility, but does not prove, that this species is preferably involved in the activation and reaction of CO. At higher temperatures, where oxygen transfer and oxidation occur, the dynamic behavior of various catalyst species may involve fast interchange of many possible intermediates. Still, in such a scenario and since species II is associated with the 1,6 and 1,11 isomers of the oxidized  $\text{H}_5\text{PV}_2\text{Mo}_{10}\text{O}_{40}$ , one may further speculate that the formation of species I occurs upon reaction of CO activated by Pd(0) with the 1,2; 1,4 and 1,5 isomers of oxidized  $\text{H}_5\text{PV}_2\text{Mo}_{10}\text{O}_{40}$ . The higher reactivity of the vicinal isomers of  $\text{H}_5\text{PV}_2\text{Mo}_{10}\text{O}_{40}$  was already previously suggested in a different reaction, the oxidation of aldehydes.<sup>23</sup> One should, however, note that calculations showed that one electron reduced forms of all the isomers of  $\text{H}_5\text{PV}_2\text{Mo}_{10}\text{O}_{40}$  have the same energy although these calculations did not consider supported species as observed in the study.<sup>16</sup>

By combining the EPR and catalytic results and based on literature precedence where it has been shown that aldehydes react with acidic polyoxometalates to yield acetals or hemiacetals,<sup>24</sup> we suggest a similar reductive activation of CO. Therefore, in Scheme 5 we show the reaction of Pd activated CO<sup>23</sup> concomitant with electron transfer at an equatorial oxygen atom of  $\text{H}_5\text{PV}_2\text{Mo}_{10}\text{O}_{40}$  where the reactive species is a vicinal isomer.<sup>25</sup> The measured vanadium–carbon distances and coupling constants for species I support such a formulation. The formulation of the EPR observed intermediate in Scheme 5 is shown as a carbonyl complex (V–CO) rather than a carboxylate complex V–C(O)OH because the conditions used to prepare samples for the EPR spectra are mild (35 °C, 10 min) and do not yield  $\text{CO}_2$  which occurs at 90 °C over 5 h.

Under anaerobic conditions and higher temperature the carbonyl complex (V–CO) yields  $\text{CO}_2$  by oxygen transfer from the polyoxometalate. Under  $\text{O}_2$  it may be assumed that oxygen could either react at the vanadium(IV) atom to yield a vanadium(V)-superoxo species or at the carbon atom to yield a peroxocarbonate species. Under acidic conditions the vanadium(V)-superoxo species would likely quickly disproportionate via second order kinetics or abstract an allylic hydrogen of 1-octene.<sup>26</sup> Since allylic oxidation products were formed only in small amounts we tend to discount this possibility. On the other hand, peroxocarbonate species previously prepared in situ from bicarbonate and  $\text{H}_2\text{O}_2$  have been reported to epoxidize alkenes and oxidize sulfides albeit at nearly neutral pH values.<sup>27</sup> It is possible or perhaps likely that Pd also plays a role in the activation of alkenes

(20) (a) Tsuji, J. *New J. Chem.* **2000**, *24*, 127–135. (b) Tsuji, J. *Acc. Chem. Res.* **1969**, *2*, 144–152. (c) Tsuji, J.; Morikawa, M.; Kiji, J. *Tetrahedron Lett.* **1963**, 1437–1440. (d) Bittler, K.; Kutepow, N. V.; Neubauer, K.; Reis, H. *Angew. Chem., Int. Ed.* **1968**, *7*, 329–335.

(21) Sheldon, R. A. *J. Mol. Catal.* **1983**, *20*, 1–26.

(22) Kao, L.-C.; Sen, A. *Chem. Commun.* **1991**, 1242–1243.

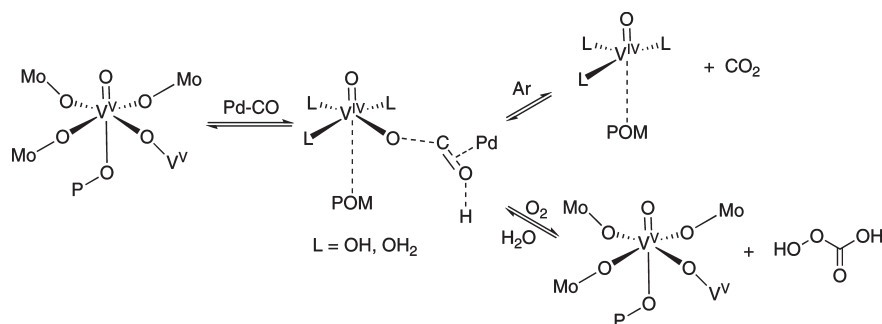
(23) Khenkin, A. M.; Rosenberger, A.; Neumann, R. *J. Catal.* **1999**, *182*, 82–91.

(24) (a) Konishi, Y.; Sakata, K.; Misono, M.; Yoneda, Y. *J. Catal.* **1982**, *77*, 169–179. (b) Popova, G. A.; Budneva, A. A.; Andrushkevich, T. V. *React. Kinet. Catal. Lett.* **1997**, *61*, 353–362.

(25) It is possible that CO is activated on a Pd(0) atom on the  $\text{Al}_2\text{O}_3$  surface or via formation of soluble Pd(0) carbonyl species.

(26) Sawyer, D. T. In *Oxygen Complexes and Oxygen Activation by Transition Metals*; Martell, A. E., Sawyer, D. T., Eds.; Plenum: New York, 1988; pp 131–148.

(27) (a) Richardson, D. E.; Yao, H.; Frank, K. M.; Bennett, D. A. *J. Am. Chem. Soc.* **2000**, *122*, 1729–1739. (b) Yao, H.; Richardson, D. E. *J. Am. Chem. Soc.* **2000**, *122*, 3220–3221. (c) Bennett, D. A.; Yao, H.; Richardson, D. E. *Inorg. Chem.* **2001**, *40*, 2996–3001.

**Scheme 5.** Suggested Pathway for the Activation of CO on Vicinal Isomers of  $\text{H}_5\text{PV}_2\text{Mo}_{10}\text{O}_{40}$  Mediated by Pd(0) and its Further Reaction under Anaerobic and Aerobic Conditions

and arenes for epoxidation and hydroxylation reactions, respectively.

### Conclusion

Carbon monoxide activated by Pd(0) was oxidized under anaerobic conditions to CO<sub>2</sub> by an electron transfer-oxygen transfer mechanism with  $\text{H}_5\text{PV}_2\text{Mo}_{10}\text{O}_{40}$  as oxygen donor. EPR and HYSCORE measurements showed the formation of two species upon reduction of  $\text{H}_5\text{PV}_2\text{Mo}_{10}\text{O}_{40}$  with <sup>13</sup>CO. Major species I (65–70%) showed coupling with hydrogen atoms of the solvent and polyoxometalate but not <sup>31</sup>P and <sup>95</sup>Mo, which together with the *g* and *A* parameters found, leads to the assignment of species I to a species resembling a vanadyl cation that probably is supported on the polyoxometalate. Additionally, the substantial <sup>13</sup>C hyperfine coupling indicates a bonding interaction with <sup>13</sup>CO. Minor species II (30–35%) showed weak axial coupling with <sup>31</sup>P (P–V distance estimated as 4.75 Å), strong equatorial coupling with <sup>95</sup>Mo, and no interaction with <sup>13</sup>C. Thus, species II is attributed to a reduced species where the vanadium(IV) atom is incorporated in the polyoxometalate framework but slightly distanced from the phosphate core that does not bind CO. Under aerobic conditions, CO/O<sub>2</sub>, the oxidation of thianthrene oxide to the sulfone rather than the disulfoxide indicates the formation of a nucleophilic oxygen donor. Oxidation reactions performed on terminal alkenes such as 1-octene yielded (~40%) nonanoic and 2-methyloctanoic acid in a 1:1 ratio as a result of hydrocarbonylation and a complicated mixture of products (~60%) that was, however, clearly a result of alkene epoxidation followed by subsequent reactions of the intermediate epoxide. One can speculate that the active oxygen donor formed may be a peroxocarbonate species.

### Experimental Section

**General Methods and Materials.** All the chemicals and solvents were purchased commercially and used without further purification. The IR spectra were measured on a Nicolet Protegé 460 FTIR; solid samples were prepared as ~3–5 wt % KBr based pellets. The <sup>31</sup>P NMR spectra were measured on a Bruker Avance DPX 500 spectrometer. Reactions were carried out in 20 mL glass pressure tubes. Products were characterized using GLC (HP-6890 gas chromatograph) with a flame ionization detector and a 30 m × 0.32 mm 5% phenylmethylsilicone (0.25 μm coating) capillary column and helium carrier gas. The products were identified using a gas chromatograph equipped with a mass-selective detector (GC-MS HP 5973) equipped with the same column. The  $\text{H}_5\text{PV}_2\text{Mo}_{10}\text{O}_{40} \cdot 34\text{H}_2\text{O}$  polyoxometalate was prepared using a known literature method.<sup>28</sup> Thermogravimetric

analysis (Mettler 50) indicated 34 water molecules per polyoxometalate unit. Elemental analysis: experimental (calculated) % P 1.31 (1.34), V 4.38 (4.41), Mo 41.32 (41.56). IR: 1057, 960, 865, and 774 cm<sup>-1</sup>. <sup>31</sup>P NMR: (CD<sub>3</sub>COCD<sub>3</sub>, 85% H<sub>3</sub>PO<sub>4</sub> external standard) δ -3.96 (6), -3.42 (1), -3.37 (4), -3.31 (2), and -3.22 (2) ppm (area of peak). <sup>18</sup>O labeled  $\text{H}_5\text{PV}_2\text{Mo}_{10}\text{O}_{40}$  (~50% enrichment) was prepared and quantified as reported.<sup>7b</sup> <sup>13</sup>CO (99% <sup>13</sup>C) was purchased from Aldrich.

**Reactions.** Reactions were carried out in Teflon lined autoclaves. In a typical reaction, 10 μmol  $\text{H}_5\text{PV}_2\text{Mo}_{10}\text{O}_{40}$  and 5% Pd/alumina (2 mg) were dissolved in 1.5 mL AcOH 90% containing 0.1 mmol NaOAc. One mmol substrate was added. CO (7 bar) and O<sub>2</sub> (3 bar) were charged, and the mixture was allowed to react under stirring at 90 °C for 15 h. After, the reaction mixture was cooled, and GC and GC-MS analyses were performed.

**EPR Measurements.** EPR samples for <sup>13</sup>CO measurements were prepared in a quartz EPR tube containing 5 mM  $\text{H}_5\text{PV}_2\text{Mo}_{10}\text{O}_{40}$  and 5% Pd/Al<sub>2</sub>O<sub>3</sub> (1 mg) in 8:1:1 AcOH:H<sub>2</sub>O:glycerol that were degassed by three pump/thaw cycles. The degassed sample was attached to a double switch lock attached to a vacuum line and a <sup>13</sup>CO lecture bottle. <sup>13</sup>CO was allowed to flow into the EPR tube. The reduced polyoxometalate (blue color) was formed under mild heating, ~35 °C, 10 min, and slow stirring. The tube was then sealed with flame. Pulse EPR measurements were carried out at 9.8 GHz and 25 K on an EleXsys E-580 Bruker spectrometer. X-band echo-detected (ED) EPR spectra were recorded using the two pulse echo with pulse durations of 16 and 32 ns and a time interval τ = 300 ns. For HYSCORE<sup>29</sup> (π/2-τ- π/2-t1-π-t2- π/2-τ- echo) the pulse durations were t<sub>π/2</sub> = 12 ns and t<sub>π</sub> = 24 ns and τ = 140 ns. The dwell time in t1 and t2 was 20 ns; 125 × 125 points were collected, and a repetition time of 4.0 ms with 3 shots per point was used. Scans were accumulated until sufficient signal-to-noise ratio was achieved. Four-step phase cycle was applied. The time domain data of HYSCORE experiments were manipulated as follows: Initially the background decay was removed by a polynomial fit, and then the data were apodized with a Sine Bell window, zero filled, and Fourier transformation was carried out after which the magnitude of the spectrum was calculated. Simulations of the ED-EPR spectrum were carried out using EasySpin.<sup>30</sup>

**Acknowledgment.** The research was supported by the German-Israeli Project Cooperation (DIP-G7.1), the Israel Science Foundation, the Kimmel Center for Molecular Design and the Ilse Katz Center for Magnetic Resonance. R.N. is the Rebecca and Israel Sieff Professor of Organic Chemistry. D.G. holds the Erich Klieger professorial chair of Chemical Physics.

**Supporting Information Available:** Additional results (Tables S1–S3) of catalytic reactions. This material is available free of charge via the Internet at <http://pubs.acs.org>.

(28) Tsigdinos, G. A.; Hallada, C. J. *Inorg. Chem.* **1968**, *7*, 437–441.

(29) Höfer, P.; Grupp, A.; Nebenführ, H.; Mehring, M. *Chem. Phys. Lett.* **1986**, *132*, 279–282.

(30) Stoll, S.; Schweiger, A. *J. Magn. Reson.* **2006**, *178*, 42–55.